Charge exchange of muons in gases. II. Application of kinetic equations to the pressure dependence of muon-spin-resonance signals

Ralph Eric Turner and Masayoshi Senba
TRIUMF, 4004 Wesbrook Mall, University of British Columbia, Vancouver, British Columbia V6T 2A3, Canada
(Received 28 September 1983)

Kinetic theory has recently been used to describe the spin dynamics associated with the stopping process encountered by highly energetic muons as they thermalize in a single-component gas. The result is a pair of rate equations that describe the dynamics encountered by the diamagnetic and paramagnetic muon species. This dynamical system has motion generated by the hyperfine interaction of the paramagnetic muon species (muonium) and by rates which are products of time-dependent rate constants for the electron-capture and -loss processes with the number density of the moderating gas. These rates are positive by definition. Using a finite-width-step-function approximation to the time dependence of the rates, analytic solutions of these equations are obtained and related to the muon spin polarization of the diamagnetic and paramagnetic species. Line shapes are obtained for the amplitudes of these polarizations as a function of the length of the charge exchange regime t_c. This time duration is inversely proportional to the number density of the moderating gas. The line shapes have two general features, namely, (i) they are constants when the duration of the charge exchange region is short (high-number densities), and (ii) they have resonances for long durations (low-number densities). Also, in general, the amplitudes of the "singlet" (muonium hyperfine frequency) term and the "triplet" (muonium Larmor frequency) term are not equal. Fits to the available experimental noble-gas data are presented using the rate constants and the time duration of the charge exchange region as parameters. The theoretical predictions suggest further experimental studies be made, in particular, to see whether the resonances are experimentally resolvable or not.

I. INTRODUCTION

In muon-spin-rotation (μSR) experiments[1] the time dependence of the spin polarization of an ensemble of thermal muons is followed by observing the ensemble of decay positrons emitted along the direction of the muon spin vectors. These experiments distinguish two general types of magnetic states associated with thermal muons, namely, paramagnetic and diamagnetic states. Chemically, the paramagnetic states are muon radicals which can be divided into two classes, namely, free muonium (Mu, the positive muon equivalence of the hydrogen atom) and molecular muon radicals. These chemical species can easily be distinguished magnetically by their characteristic Larmor frequencies. In contrast, with present experimental techniques in μSR, no distinction can be made between the characteristic Larmor frequencies of chemical species containing the muon in a diamagnetic environment. Examples of classes of such chemical species involving the muon are neutral molecules, molecular ions, and of course, the bare muon itself. Since molecular muon radicals have not been found in gas-phase experiments, then only two magnetic states are observed, namely, the paramagnetic state which chemically is muonium and the diamagnetic state which may be a single chemical species or a set of different chemical species. Throughout this paper the term "state" will be used to describe the spin environment of the muon, while "species" will be used to denote its chemical environment.

Generally, the time resolution of these experiments is of the order of tens of nanoseconds as is the time scale[2] of the stopping process for the incoming highly energetic muons. Thus the outcome of the stopping process acts as the initial conditions for the experiments. Therefore it is of interest to have a theoretical basis for understanding the effects that the thermalization of the translational motion has on the spin dynamics. Such a description has recently been presented[3] based upon kinetic theory. The result is a pair of rate equations for the diamagnetic and paramagnetic spin states. The effect of this stopping process is completely contained in the (positive) time-dependent rate superoperators that describe the collision processes which interconvert the two spin states. These rate superoperators depict loss of an electron from muonium to form a diamagnetic chemical species and capture of an electron by a diamagnetic species to form muonium. They contain contributions from all possible chemical species that may be involved and are averages of the product of the total cross sections for the appropriate collision with density operators that describe the translational motion of the moderating gas and the chemical species containing the muon. Their time dependence is determined by the time dependence associated with the thermalization of the kinetic energy of the muon, that is, the density operator which describes the translational motion of the chemical species containing the muon. These translational density operators give the probability that the chemical species will have a certain kinetic energy at a certain time. On the other hand, the moderating gas is assumed to be in thermal equilibrium and, thus, is

described by a product of time-independent equilibrium Maxwell-Boltzmann density operators, one for each gas atom.

In this stopping process three main regions are encountered before thermalization, that is, the Bethe-Bloch region from $t=0$ to t_1, the charge exchange region from t_1 to t_2 ($t_c=t_2-t_1$), and the epithermal region from t_2 to the beginning of the thermal regime which starts at t_T. It is this last time which acts as the initial time for the experiments. In the Bethe-Bloch region, where the dominant process is ionization of the moderating gas, the muon remains as a bare muon. Thus the spin dynamics is simply that of a free diamagnetic state. Indeed, it is constant since the time scale of this region is many orders of magnitude faster than the period of the diamagnetic Larmor frequency. In terms of the rate equations this means that there is an energy mismatch between the total cross sections and the kinetic energy of the muon which results in both the rate superoperators being zero. On the other hand, in the charge exchange region, both processes are occurring simultaneously. Thus the rates for electron capture and loss are both positive and nonzero. Elastic and inelastic scattering also occurs in this region. Indeed, these latter processes dominate the third or epithermal region where one of the rates may be nonzero, but not both. However, by the end of the epithermal region, both rates must be zero since, for large number densities, there is no depolarization of the signals. Such a condition holds because nonzero rates up to and including thermal times would lead to noncoherent depolarization of the muon ensemble.

The purpose of the present paper is twofold. First, Laplace transforms are used to obtain explicit solutions of these equations based upon an approximation to the rates. That is, the rates are assumed to be zero during the Bethe-Bloch regime from $t=0$ to t_1, to be nonzero but independent of time for the duration of the charge exchange regime from t_1 to t_2, and zero again during the epithermal region from t_2 to t_T. This replaces the exact time dependencies of the rates, namely, zero initially, positive and nonzero as time progresses, and zero again at time t_T, with finite-width-step functions of different heights. The time windows or widths of the capture and loss rates are assumed to be the same, that is, they are taken to be the duration t_c of the charge exchange region. Such a seemingly simple approximation leads to nontrivial predictions for the line shapes of the amplitudes of the polarization of the muon. Thus its validity can easily be tested experimentally. If, indeed, it proves to be inadequate then more realistic approximations will have to be considered. However, solutions of the exact rate equations require solutions of translational Boltzmann equations for each chemical species since the time dependence of each rate superoperator is explicitly contained in the appropriate translational density operators. Such a calculation is beyond the scope of present-day theoretical techniques.

The second purpose of this paper is to explore the consequences that these solutions have for the observed diamagnetic and paramagnetic signals as a function of the number density n of the moderating gas. The number density enters the rate equations in two ways, that is, through the rates themselves and through the time duration of the charge exchange regime which is inversely proportional to n. In particular, the line shapes associated with the amplitudes of the polarization of the muon in the diamagnetic and paramagnetic states have two general features as a function of the time duration of the charge exchange regime, namely (i) they are constants for high number densities and (ii) they exhibit resonances at low number densities. For the first region (high number densities) there is no depolarization, that is, the sum of the amplitudes is equal to the total incoming amplitude. This agrees with experimental results[2,4,5] and is in contrast to the situation[1,6–8] in condensed phases where there is, in general, a significant depolarization. For example, in liquid water there is a 20% lost fraction. The theoretical description of the gas-phase experiments is based upon two assumptions, namely (i) that only binary collisions occur and (ii) that no subsequent interactions occur between the muon and the products of a prior collision. This implies that the lost fractions in liquids and solids may have three possible sources, that is (i) many-body effects such as collective modes and/or many-body collisions, (ii) interactions with products of prior collisions, and (iii) interactions with short-lived species not present in the gas phase (for example, solvated electrons). On the other hand, depolarization does occur in the second region of interest, namely, low-density gases. The mechanism for depolarization in this regime is due to the hyperfine interaction and the cyclic nature of the charge exchange process. In particular, when a collision forms muonium, exchange of polarization between the muon spin and the electron spin can occur during free flight. This exchange is due to the hyperfine interaction. If the time between collisions is much shorter than the period of a hyperfine oscillation then the electron will not carry away any appreciable polarization when it is stripped from the muon in the next charge-transfer collision. For dense gases no transfer of polarization occurs over the whole charge exchange region. On the other hand, for low-density gases the time between collisions near the end of the region becomes an appreciable fraction of the period of the hyperfine interaction. Thus, stripped electrons can carry away an appreciable amount of the muon's original polarization. Indeed, there will be a density where the time between collisions will be such that an electron will be lost when it has acquired all the muon's polarization. At lower densities still the electron will have acquired all the polarization and will be exchanging some of it back to the muon when it is stripped by the next charge-transfer collision. This is the source of the resonances that the theory predicts. However, the size of these resonances depends upon how much polarization has already been lost before such "restoring" events can occur. The real parts of the poles associated with the inverse Laplace transforms of the rate equations lead to exponential damping of the resonances while the periods of these resonances are given by the imaginary parts. Such resonances have as yet to be experimentally observed. Indeed the parameters may be such that the resonances are too small in height to be seen. Such extreme damping is most likely to occur when the muon spends most of its time as muonium rather than as

a diamagnetic muon species during the charge exchange regime. Also, in general, the amplitudes of the hyperfine frequency term ("singlet" signal) and the muonium Larmor frequency term ("triplet" signal) are not equal. This arises since the muonium hyperfine frequency enters the rate equations in an asymmetric fashion. That is, the muonium hyperfine frequency only appears in the equations for the singlet components of the spin density operators and does not appear in the equations for the triplet components, see Eqs. (3.2) and (3.16). However, for rates large compared to the hyperfine frequency, for example, at high densities, these amplitudes become equal. At present, the hyperfine frequency signal is not observed experimentally while it has been assumed that the amplitudes associated with the muonium hyperfine frequency and the muonium Larmor frequency are equal.[3]

The rate equations and their associations with the observed thermal signals are reviewed in Sec. II. Explicit solutions of the rate equations are obtained and related to the diamagnetic and paramagnetic signals in Sec. III. High number-density limits of these expressions are presented in Sec. IV, while large rate-constant results are given in Sec. V. Finally, fits to the available noble-gas data are presented in Sec. VI.

II. RATE EQUATIONS

For the typical muon-spin-rotation (μSR) experiment in gases,[1] the muon beam enters the target with its momentum and spin polarization perpendicular to the applied external magnetic field. By definition this external field is in the z direction while the initial momentum is in the y direction. Observation of the positrons emitted by the decaying muons is made in either the positive or negative x directions. The components of the spin density operator which describe the bare diamagnetic muons as they enter the target are as follows: $\rho^{\mu}_{\alpha\alpha}(0)=\frac{1}{2}(1+P^z_\mu)$, $\rho^{\mu}_{\beta\beta}(0)=\frac{1}{2}(1-P^z_\mu)$, and $\rho^{\mu}_{\alpha\beta}(0)=\frac{1}{2}\,|P_\mu|\exp(i\varphi_\mu)=\rho^{\mu}_{\beta\alpha}(0)^*$, where α and β are the $+\frac{1}{2}$ and $-\frac{1}{2}$ spin states in the field direction. They involve the initial polarizations in the z direction P^z_μ, in the x direction $|P_\mu|\cos(\varphi_\mu)$, and in the y direction $|P_\mu|\sin(\varphi_\mu)$. Standard[1] experimental conditions are $P^z_\mu\approx 0$ and $\varphi_\mu\approx -\pi/2$. On the other hand, since the moderating gas is assumed to be in thermal equilibrium, then the electrons which it donates to the charge exchange regime will be unpolarized. Thus the initial or equilibrium components of the electronic density operator are $\rho^{e}_{\alpha\alpha}=\rho^{e}_{\beta\beta}=\frac{1}{2}$ and $\rho^{e}_{\alpha\beta}=\rho^{e}_{\beta\alpha}=0$. The initial muonium spin density operator is zero since there is no muonium present before the charge exchange region begins.

The derivation[3] of the rate equations begins with the exact quantal $(N+1)$-particle Liouville equation for the single-component gas and the muon. Two first-order quantal Bogoliubov-Born-Green-Kirkwood-Yvon (BBGKY) equations[9] for the diamagnetic and paramagnetic muon species are then obtained by averaging over all the gas particles. These equations for the single-particle-reduced density operators are, of course, not closed as they involve two-particle-reduced density operators for a gas particle and either a diamagnetic or paramagnetic muon species. To close these equations the generalized Boltzmann ansatz[9] is invoked, that is, the two-particle-reduced density operators are written as products of the appropriate Moller superoperators and the single-particle-reduced density operators for the gas particle and the muon species. The result is a set of coupled quantal Boltzmann equations for the paramagnetic muon species, namely, muonium, and the various diamagnetic chemical species which contain the muon. These equations involve both the translation and spin degrees of freedom. The translational degrees of freedom are then traced over and the diamagnetic species summed over to produce a pair of rate equations whose dynamics is generated by the free-flight spin Liouville superoperators and by the time-dependent rate superoperators which depict the electron-capture and -loss processes, that is,

$$\begin{aligned}\frac{d\rho_\mu(t)}{dt}+i\mathscr{L}_\mu\rho_\mu(t)&=-R_C(t)\mathscr{P}_{e,eq}\,\rho_\mu(t)+R_L(t)\rho_{\mathrm{Mu}}(t)\,,\\ \frac{d\rho_{\mathrm{Mu}}(t)}{dt}+i\mathscr{L}_{\mathrm{Mu}}\rho_{\mathrm{Mu}}(t)&=-R_L(t)\rho_{\mathrm{Mu}}(t)\\ &\quad+R_C(t)\mathscr{P}_{e,eq}\,\rho_\mu(t)\,,\end{aligned}\tag{2.1}$$

where $R_C(t)=nK_C(t)$ and $R_L(t)=nK_L(t)$ are the rates of electron capture and loss, respectively. They are the products of the number density of the moderating gas and the appropriate time-dependent rate constants $K_C(t)$ and $K_L(t)$. For example, the capture rate constant is given by a sum over the individual rate constants[3] for each diamagnetic chemical species, namely,

$$\begin{aligned}K_C(t)=\int d\vec{\mathrm{P}}^{\,cm}_{\mu 1}\int d\vec{\mathrm{p}}^{\,\mathrm{rel}}_{\mu 1}\sigma_{\mathrm{tot}}(\mu\rightarrow\mathrm{Mu})(p^{\mathrm{rel}}_{\mu 1}/m_{\mu 1})\\ \times f_1(M_1\vec{\mathrm{P}}^{\,cm}_{\mu 1}/M_{\mu 1}-\vec{\mathrm{p}}^{\,\mathrm{rel}}_{\mu 1})\\ \times f_\mu(M_\mu\vec{\mathrm{P}}^{\,cm}_{\mu 1}/M_{\mu 1}+\vec{\mathrm{p}}^{\,\mathrm{rel}}_{\mu 1}\,|\,t)\,.\end{aligned}\tag{2.2}$$

Here f_1 is the Maxwell-Boltzmann momentum distribution[10] for the translational motion of an equilibrium gas particle, while f_μ is the momentum distribution associated with the time-dependent single-particle translational muon reduced density operator. $\sigma_{\mathrm{tot}}(\mu\rightarrow\mathrm{Mu})$ is the total cross section[11] for scattering events that begin with a diamagnetic muon species and end with muonium. A similar expression holds for the electron-loss process. Here these time-dependent rate constants are replaced by the product of time-independent parameters, namely, K_C and K_L, and a finite-width-step function of the time duration of the charge exchange region.

The free-flight muon spin dynamics is generated by the diamagnetic muon Liouville superoperator, $\mathscr{L}_\mu=\hbar^{-1}[H_\mu,\ldots]_-$, which is $\hbar^{-1}$ times the commutator with the muon spin Hamiltonian[1] $H_\mu=-\omega_\mu\vec{\mathrm{I}}\cdot\hat{Z}$, where $\omega_\mu=8.6\times10^4 B/\mathrm{sec}$ is the diamagnetic muon Larmor frequency. Similarly, free-flight muonium spin dynamics is generated by the paramagnetic muonium Liouville superoperator, $\mathscr{L}_{\mathrm{Mu}}=\hbar^{-1}[H_{\mathrm{Mu}},\ldots]_-$, which is $\hbar^{-1}$ times the commutator with the muonium spin Hamiltonian[1] $H_{\mathrm{Mu}}=\omega_e\vec{\mathrm{S}}\cdot\hat{Z}-\omega_\mu\vec{\mathrm{I}}\cdot\hat{Z}+\hbar^{-1}\omega_0\vec{\mathrm{I}}\cdot\vec{\mathrm{S}}$. Here ω_e is the electronic Larmor frequency, while ω_0 is the muonium hyperfine frequency 2.8×10^{10} rad/sec. The rate equations are solved in Sec. III using the eigenfunctions[1] of the

muonium spin Hamiltonian, namely, $|1\rangle=|\alpha\alpha\rangle$, $|2\rangle=s|\alpha\beta\rangle+c|\beta\alpha\rangle$, $|3\rangle=|\beta\beta\rangle$, and $|4\rangle=c|\alpha\beta\rangle-s|\beta\alpha\rangle$, where the first spin is that of the muon. The normalization constants $c=\{\frac{1}{2}[1+x/(1+x^2)^{1/2}]\}^{1/2}$ and $s=(1-c^2)^{1/2}$ involve a field-strength parameter $x=(\omega_e+\omega_\mu)/\omega_0=6.3\times10^{-4}B$. Also associated with this muonium spin Hamiltonian is the muonium Larmor frequency $\omega_{\mathrm{Mu}}=(\omega_e-\omega_\mu)=8.8\times10^6B/\mathrm{sec}$. Finally, these rate equations involve a multiplication superoperator which selects the spin state of the electrons that are captured by the muon in the formation of muonium. This superoperator represents multiplication by the equilibrium electron spin density operator and is diagonal in the $\alpha\alpha$ basis, namely,

$$\langle\langle\,|ab\rangle\langle cd|\,|\mathscr{P}_{e,eq}=\rho^e_{bd}\langle\langle\,|ab\rangle\langle cd|\,|\,, \tag{2.3}$$

where the double bracket notation[12] is used to distinguish the operator space from the standard wave function space.

Solutions of these rate equations evaluated at the end of the charge exchange region act as the initial conditions for the epithermal and thermal regions where it is assumed, for noble gases, that spin-lattice-type relaxations and the free-flight spin Hamiltonians are adequate to describe the spin dynamics. For comparison with the experimental noble-gas signals, the rates K_C and K_L and the duration of the charge exchange regime $t_c=t_2-t_1$ are treated as parameters in a fitting procedure. This time span $t_c=\sum_{i=1}^{N_c}\omega_c^i$ can be written[13] in terms of the total number of collisions N_c occurring during the regime and the collision frequency $\omega_c^i=(nv_i\sigma_i)^{-1}$. Here v_i is the average free-flight velocity between collision i and $i+1$, while σ_i is the total cross section associated with v_i. Therefore the time duration of the region can be written as $t_c=\tau_c/n$. Thus this theory involves three fitting parameters K_C, K_L, and τ_c. On the other hand, the number density acts as an experimentally adjustable quantity.

In gaseous μSR experiments time histograms of the diamagnetic muon and paramagnetic muonium Larmor precessions are observed.[1] The time scale of these histograms is microseconds, that is, thermal times. Times on the order of nanoseconds are too short to be observed and their time zero is of the order of the start of the thermal region. These histograms are fit to functional form[1]

$$N(t)=N_0\exp(-t/\tau_\mu)[1+S(t)]+B\,, \tag{2.4}$$

where N_0 is a normalization, $\tau_\mu=2.197$ μsec is the muon lifetime, B is a time-independent background, and $S(t)$ is the thermal signal

$$S(t)=A_\mu\exp(-\lambda_\mu t)\cos(\omega_\mu t+\theta_\mu)+\sum_{i=1}^{4}A^i_{\mathrm{Mu}}\exp(-\lambda^i_{\mathrm{Mu}}t)\cos(\omega_i t-\theta^i_{\mathrm{Mu}})\,. \tag{2.5}$$

Here λ_μ and λ^i_{Mu} are the spin-lattice relaxation rates for the diamagnetic muon and paramagnetic muonium states, while A_μ and A^i_{Mu} are their amplitudes and θ_μ and θ^i_{Mu} are their phases. The paramagnetic frequencies are those associated with the allowed transitions in a transverse magnetic field of the muonium Breit-Rabi diagram,[1] namely, $\omega_1=\omega_{\mathrm{Mu}}+\Omega$, $\omega_2=\omega_{\mathrm{Mu}}-\Omega$, $\omega_3=\omega_0+\omega_{\mathrm{Mu}}+\Omega$, and $\omega_4=\omega_0-\omega_{\mathrm{Mu}}+\Omega$, where $\Omega=\frac{1}{2}\omega_0[(1+x^2)^{1/2}-1]$ is a field-dependent beat frequency. However, the hyperfine signals are not observed experimentally as their time scale is of the order of tenths of a nanosecond. The signal $S(t)$ is, in fact, the expectation value of the polarization of the muon spin vector $\vec{I}$ in the X direction, namely,

$$S(t)=\langle P_\chi\rangle_\rho(t)=\mathrm{Tr}[(2/\hbar)\vec{I}\cdot\hat{X}\rho(t)]\,, \tag{2.6}$$

where $\rho(t)$ is the appropriate thermal spin density operator for the diamagnetic and paramagnetic muon states. For comparison of different experimental results, normalized signals are considered here, that is, $S(t)$ divided by the amplitude of the incoming polarization. In gas-phase experiments[1,2] this incoming amplitude is obtained by measuring the diamagnetic signal produced when an aluminum plate (*in vacuo*) replaces the target gas. No depolarization of the beam occurs and no muonium is formed in aluminum and, thus, the incoming amplitude is termed the aluminum asymmetry.[1,2] Corrections for the wall signals[2] should also be included in the experimental amplitudes as well. From now on the term "amplitude" is taken to be synonymous with the wall corrected experimental amplitude divided by the aluminum asymmetry, that is, the normalized amplitude.

From a theoretical view point[3] the signal $S(t)$ becomes a sum of diamagnetic and paramagnetic terms, namely,

$$S(t)=\mathrm{Tr}[P_X\rho(t)]/|P_\mu|=P^\mu_X(t)+P^{\mathrm{Mu}}_X(t)\,, \tag{2.7}$$

where the density operators used to evaluate $P^\mu_X(t)$ and $P^{\mathrm{Mu}}_X(t)$ have motion generated by the appropriate Liouville spin superoperators along with the thermal spin-lattice relaxation rates. The initial conditions of these density operators are given by the solutions of the rate equations evaluated at t_c. Thus the diamagnetic and paramagnetic contributions are

$$P^\mu_X(t)=P_\mu\exp[-\lambda_\mu(t-t_T)]\cos[\omega_\mu(t-t_T)+\theta_\mu]\,,$$

and

$$P^{\mathrm{Mu}}_X(t)=\sum_{i=1}^{4}P^i_{\mathrm{Mu}}\exp[-\lambda_{\mathrm{Mu}}(t-t_T)]\cos[\omega_i(t-t_T)-\theta^i_{\mathrm{Mu}}]\,. \tag{2.8}$$

The phases of these expressions are simply the phases of the experimental signal, Eq. (2.5), while the amplitudes P_μ and P^i_{Mu} are the appropriate normalized (wall-corrected) amplitudes. The diamagnetic term involves the amplitude

$$P_\mu=|\rho_\alpha(t_c)+\rho_a(t_c)|\,, \tag{2.9}$$

and its associated phase. Here the density matrix elements are components of the diamagnetic spin density operator described by Eq. (2.1), namely,

$$\rho_\alpha(t_c)=2[c\rho^\mu_{12}(t_c)-s\rho^\mu_{14}(t_c)]\,,$$
$$\rho_a(t_c)=2\,|\,s\rho^\mu_{23}(t_c)+c\rho^\mu_{43}(t_c)\,|\,. \tag{2.10}$$

On the other hand, the paramagnetic amplitudes are given by

$$P^1_{\rm Mu}=|\rho_1(t_c)|=|2s\rho^{\rm Mu}_{23}(t_c)|\ ,$$
$$P^2_{\rm Mu}=|\rho_2(t_c)|=|2c\rho^{\rm Mu}_{12}(t_c)|\ ,$$
$$P^3_{\rm Mu}=|\rho_3(t_c)|=|-2s\rho^{\rm Mu}_{14}(t_c)|\ , \qquad (2.11)$$
$$P^4_{\rm Mu}=|\rho_4(t_c)|=|2c\rho^{\rm Mu}_{43}(t_c)|\ ,$$

while the phases are defined accordingly. In principle there are five signals of different frequencies that can be observed if x is of sufficient size that Ω is resolvable and if the time resolution of the experiment is sufficient to resolve the hyperfine frequency. As pointed out, the latter signals are not currently observed, while in gases it is standard experimental practice[2] to measure the muonium signal at low fields (about 7 G) and the diamagnetic signal at intermediate fields (typically 70—300 G). Thus only two signals are currently observed, namely, that associated with the diamagnetic Larmor frequency and that with the paramagnetic muonium Larmor frequency. The muonium signal is the Larmor part of the low field muonium polarization

$$P^{\rm Mu}_X(t)=P_{\rm Mu}\cos(\omega_{\rm Mu}t-\theta_{\rm Mu})+P^0_{\rm Mu}\cos(\omega_0 t-\theta^0_{\rm Mu}), \qquad (2.12)$$

where

$$P_{\rm Mu}=|\rho_1(t_c)+\rho_2(t_c)|\ ,\quad P^0_{\rm Mu}=|\rho_3(t_c)+\rho_4(t_c)|\ , \qquad (2.13)$$

are the amplitudes of the "triplet" or muonium Larmor frequency term and the "singlet" or hyperfine term. The phases associated with these amplitudes are simply the phases associated with the appropriate combination of matrix elements. Experimentally measured quantities are then the amplitudes P_μ and $P_{\rm Mu}$ and the phases θ_μ and $\theta_{\rm Mu}$, cf. Eq. (2.5). It is also of interest to define the fractions

$$F_\mu=P_\mu/P_T,\quad F_{\rm Mu}=\sum_{i=1}^{4}P^i_{\rm Mu}/P_T=1-F_\mu \qquad (2.14)$$

of muon and muonium, respectively, where P_T is the sum of the diamagnetic and paramagnetic amplitudes $P_\mu+\sum_{i=1}^4 P^i_{\rm Mu}(\le 1)$. Expressions for the various amplitudes and phases are evaluated in Sec. III in terms of the analytic solutions of the rate equations which describe the spin dynamics that emerge from the charge exchange region. The resulting signals are then fitted to the noble-gas data which are functions of the number density (pressure) of the moderating gas.

III. DIAMAGNETIC AND PARAMAGENTIC THEORETICAL SIGNALS

The rate equations with time-independent rate constants are now solved using the muonium basis. In this representation the α, 2, and 3 matrix elements couple together as do the a, 1, and 4 components. There is no coupling between these two sets. The former is considered first.

A. "Two" and "three" paramagnetic signals

The 1 eigenstate couples to the 2 and 4 eigenstates through the muon spin density operator and the equilibrium electron spin density operator in Eqs. (2.1). That is,

$$\langle\langle\,|1\rangle\langle 2|\,|\mathscr{P}_{e,eq}\,|\rho_\mu(t)\rangle\rangle=\tfrac{1}{2}[c^2\rho^\mu_{12}(t)-sc\rho^\mu_{14}(t)]=c\rho_\alpha(t)/4$$
and (3.1)
$$\langle\langle\,|1\rangle\langle 4|\,|\mathscr{P}_{e,eq}\,|\rho_\mu(t)\rangle\rangle=\tfrac{1}{2}[-sc\rho^\mu_{12}(t)+s^2\rho^\mu_{14}(t)]$$
$$=-s\rho_\alpha(t)/4\ ,$$

where use has been made of Eq. (2.3) and the representation of the muonium eigenstates in terms of the $\alpha\alpha$ basis. Thus the rate equations (2.1) which couple the paramagnetic and diamagnetic components of the spin density operator become three linear coupled differential equations which describe the dynamics associated with the α, 2, and 3 matrix elements, namely,

$$d\rho_\alpha(t)/dt=-\tfrac{1}{2}R_C\rho_\alpha(t)+R_L[\rho_2(t)+\rho_3(t)]\ ,$$
$$d\rho_2(t)/dt=-R_L\rho_2(t)+\tfrac{1}{2}R_Cc^2\rho_\alpha(t)\ , \qquad (3.2)$$
$$d\rho_3(t)/dt=-(R_L+i\omega_0)\rho_3(t)+\tfrac{1}{2}R_Cs^2\rho_\alpha(t)$$

and are subject to the following initial conditions: $\rho_\alpha(t_1)=\frac{1}{2}\exp(i\varphi_\mu)$, $\rho_2(t_1)=\rho_3(t_1)=0$.

Using Laplace transforms,

$$\bar\rho_i=\int_{t_1}^{\infty}dt\exp[-xR_S(t-t_1)]\rho_i(t)\ , \qquad (3.3)$$

Eqs. (3.2) can be transformed into the following set of three coupled algebraic equations:

$$(x+f_\mu)\bar\rho_\alpha=\rho_\alpha(t_1)/R_s+f_\mu(\bar\rho_2+\bar\rho_3)\ ,$$
$$(x+f_\mu)\bar\rho_2=f_{\rm Mu}c^2\bar\rho_\alpha\ , \qquad (3.4)$$
$$[x+f_\mu+i(\omega_0/R_S)]\bar\rho_3=+s^2f_{\rm Mu}\bar\rho_\alpha\ ,$$

where $R_S=R_L+\frac{1}{2}R_C=nK_S$ is the total rate and where $f_\mu=R_L/R_S=K_L/K_S$ and $f_{\rm Mu}=\frac{1}{2}R_C/R_S=\frac{1}{2}K_C/K_S$ are the fractions of diamagnetic muon and muonium, respectively, which emerge at high pressures, see Sec. IV, where the time duration of the charge exchange regime is short compared to the hyperfine interaction. The solutions of Eqs. (3.4),

$$\bar\rho_2=\bar\rho_\alpha[f_{\rm Mu}c^2/(x+f_\mu)]\ ,$$
$$\bar\rho_2=\bar\rho_\alpha\{+f_{\rm Mu}s^2/[x+f_\mu+i(\omega_0/R_S)]\}\ , \qquad (3.5)$$
$$\bar\rho_\alpha=\rho_\alpha(t_1)\left[(x+f_\mu)[x+f_\mu+i(\omega_0/R_S)]\Big/\prod_{i=1}^{3}(x-x_{S,i})\right]\Big/R_S,$$

involve the roots of a cubic equation with complex coefficients, namely,

$$0=x^3_{S,i}+x^2_{S,i}[1+f_\mu+i(\omega_0/R_S)]$$
$$+x_{S,i}[f_\mu+i(\omega_0/R_S)]+is^2f_\mu f_{\rm Mu}(\omega_0/R_S)\ . \qquad (3.6)$$

This cubic equation has three complex roots, $x_{S,i}=-\lambda_{S,i}+i\nu_{S,i}$, which can be written in terms of three (positive) relaxation rates, $\lambda_{S,i}$, and three associated frequencies, $\nu_{S,i}$. The relaxation rates lead to exponential damping of the amplitudes, while the frequencies lead to sinusoidal oscillations.

Inverting the Laplace transforms leads to analytic expressions for the various matrix elements of the spin density operators. For example, at the end of the charge exchange region the 2 matrix element becomes

$$\rho_2(t_c)=\tfrac{1}{2}f_{\mathrm{Mu}}c^2\sum_{i=1}^{3}\exp(x_{S,i}R_S t_c+i\varphi_\mu)[x_{S,i}+f_\mu+i(\omega_0/R_S)]\left[\prod_{j\neq i}(x_{S,i}-x_{S,j})\right]^{-1}$$
$$=\tfrac{1}{2}f_{\mathrm{Mu}}c^2\sum_{i=1}^{3}\exp[(-\lambda_{S,i}+i\nu_{S,i})K_S\tau_c+i(b_{S,i}+\varphi_\mu)]B_{S,i}=P_{\mathrm{Mu}}^2\exp(i\theta_{\mathrm{Mu}}^2)\ . \tag{3.7}$$

The next to the last form of Eq. (3.7) involves a real amplitude function and a frequency, namely,

$$B_{S,i}=D_{S,i}/E_{S,i},\quad b_{S,i}=d_{S,i}-e_{S,i}\ , \tag{3.8}$$

respectively. These expressions are related to the relaxation rates and frequencies by the following formulas:

$$x_{S,i}+f_\mu+i\omega_0/R_S=D_{S,i}\exp(id_{S,i})\ ,$$
$$x_{S,i}-x_{S,j}=E_{S,ij}\exp(ie_{S,ij})\ , \tag{3.9}$$
$$E_{S,i}=\prod_{j\neq i}E_{S,ij},\quad e_{S,i}=\sum_{j\neq i}e_{S,ij}\ .$$

It is to be noted that the explicit dependence on the number density of the moderating gas has been isolated in the relaxation rates, their associated frequencies, and the D functions. The E and B functions implicitly depend on n through the complex roots of Eq. (3.6).

As with the "two" paramagnetic signal the amplitude of the "three" signal is the magnitude of the 3 matrix element. That is,

$$P_{\mathrm{Mu}}^3=[\tfrac{1}{2}f_{\mathrm{Mu}}s^2]\left[\sum_{i=1}^{3}\exp(-2\lambda_{S,i}K_S\tau_c)C_{S,i}{}^2+2\sum_{j\neq i}\exp[-(\lambda_{S,i}+\lambda_{S,j})K_S\tau_c]C_{S,i}C_{S,j}\right.$$
$$\left.\times\cos[(\nu_{S,i}-\nu_{S,j})K_S\tau_c+(c_{S,i}-c_{S,j})]\right]^{1/2}\ , \tag{3.10}$$

while its corresponding phase is $\theta_{\mathrm{Mu}}^3=\varphi_\mu+\arg[\rho_3(t_c)]$. Here the real amplitude and phase functions

$$C_{S,i}=F_{S,i}/E_{S,i},\quad c_{S,i}=f_{S,i}-e_{S,i} \tag{3.11}$$

involve the complex function

$$x_{S,i}+f_\mu=F_{S,i}\exp(if_{S,i}) \tag{3.12}$$

and the previously defined E functions, Eq. (3.9). Finally, the α component of the spin density matrix becomes

$$\rho_\alpha(t_c)=\tfrac{1}{2}\sum_{i=1}^{3}\exp[(-\lambda_{S,i}+i\nu_{S,i})K_S\tau_c+i(a_{S,i}+\varphi_\mu)]A_{S,i}\ , \tag{3.13}$$

where

$$A_{S,i}=D_{S,i}F_{S,i}/E_{S,i},\quad a_{S,i}=d_{S,i}+f_{S,i}-e_{S,i}\ . \tag{3.14}$$

This matrix element is related to the diamagnetic signal, see Eqs. (2.5)–(2.9).

These expressions for the amplitudes and phases of the μSR signals are evaluated for high number densities in Sec. IV and for large rate constants in Sec. V. The "one" and "four" paramagnetic signals are considered next.

B. "One" and "four" paramagnetic signals

The 3 eigenstate also couples to the 2 and 4 eigenstates through the muon spin density operator and the equilibrium electron spin density operator in Eq. (2.1). That is,

$$\langle\langle\,|2\rangle\langle 3||\mathscr{P}_{e,eq}\,|\rho_\mu(t)\rangle\rangle$$
$$=\tfrac{1}{2}[s^2\rho_{23}^\mu(t)+sc\rho_{43}^\mu(t)]=s\rho_a(t)/4$$

and

$$\langle\langle\,|4\rangle\langle 3||\mathscr{P}_{e,eq}\,|\rho_\mu(t)\rangle\rangle$$
$$=\tfrac{1}{2}[sc\rho_{23}^\mu(t)+c^2\rho_{43}^\mu(t)]=c\rho_a(t)/4\ . \tag{3.15}$$

The a, 1, and 4 components of the density operators satisfy the following set of three coupled linear first-order differential equations:

$$d\rho_a(t)/dt=-\tfrac{1}{2}R_C\rho_a(t)+R_L[\rho_1(t)+\rho_4(t)]\ ,$$
$$d\rho_1(t)/dt=-R_L\rho_1(t)+\tfrac{1}{2}R_C s^2\rho_a(t)\ , \tag{3.16}$$
$$d\rho_4(t)/dt=-(R_L-i\omega_0)\rho_4(t)+\tfrac{1}{2}R_C c^2\rho_a(t)\ .$$

These equations are complex conjugates of Eqs. (3.2) with s and c interchanged. Indeed, for low fields where $s=c$ they are simply complex conjugates of each other. Solutions to this set of equations follow directly from Sec. III A except that the cubic equation

$$0=x_{C,i}^3+x_{C,i}^2[1+f_\mu-i(\omega_0/R_S)]$$
$$+x_{C,i}[f_\mu-i(\omega_0/R_S)]-ic^2f_\mu f_{\mathrm{Mu}}(\omega_0/R_S) \tag{3.17}$$

replaces Eq. (3.6). The roots $x_{C,i}=-\lambda_{C,i}-i\nu_{C,i}$, of this equation are complex conjugates of the previous roots with s replaced by c. For low fields where s and c are equal, the two sets of roots are simply complex conjugates of each other. The "one" signal has the same form as the "two" signal except that c replaces s everywhere. That is, the B and b functions are evaluated using the c roots. Similar results hold for the "four" and "three" signals and the a and α components of the density operator.

C. Diamagnetic and low-field paramagnetic signals

The amplitude of the normalized observed diamagnetic muon signal is simply given by the magnitude of the sum of the α component and the a component of the spin density operators, namely,

$$P_\mu=\tfrac{1}{2}\left|\sum_{i=1}^{3}\{\exp[(-\lambda_{S,i}+i\nu_{S,i})K_S\tau_c+ia_{S,i}]A_{S,i}+\exp[(-\lambda_{C,i}-i\nu_{C,i})K_S\tau_c-ia_{C,i}]A_{C,i}\}\right| . \tag{3.18}$$

The phase follows accordingly. This signal is typically measured between 70 and 300 G where there is a nontrivial difference between the two sets of roots. On the other hand, the paramagnetic signal is usually measured at low fields (around 7 G) where $s=c$. Thus the roots are simply complex conjugates of each other, namely, $\lambda_{C,i}=\lambda_{S,i}=\lambda_i$ and $\nu_{C,i}=\nu_{S,i}=\nu_i$. Also, Ω is not resolvable at these low fields. Thus the muonium Larmor signal, Eq. (2.13), is of the form

$$P_{\mathrm{Mu}}=\tfrac{1}{2}(f_{\mathrm{Mu}})\left|\sum_{i=1}^{3}B_i\exp(-\lambda_iK_S\tau_c)\cos(\nu_iK_S\tau_c+b_i)\right| , \tag{3.19}$$

where the B functions are evaluated using the above low-field roots. A similar expression holds for the hyperfine signal.

IV. HIGH NUMBER-DENSITY EXPRESSIONS

When the number density of the moderating gas is high and when the rate constants K_S are of the order of or greater than the hyperfine frequency, then $(\omega_0/R_S)=(\omega_0/nK_S)$ is a small parameter. Simple expressions for the relaxation rates and their associated frequencies can then be obtained in terms of a power series in (ω_0/R_S). Since the number-density dependence of the amplitudes resides completely within these relaxation rates and frequencies and the D functions then to zeroth order in (ω_0/R_S), the line shapes are independent of the number density of the moderating gas. That is, there is a high number-denisty limit of the amplitudes in the gas-phase experiments. In particular, to zeroth order in (ω_0/R_S), the s and c roots become real and equal, namely, $\lambda_1=0$, $\lambda_2=f_\mu$, $\lambda_3=1$. Since $D_2=F_2=0$ then the contribution of the second root to the normalized amplitudes is zero, while the remaining roots give

$$P^1_{\mathrm{Mu}}=P^3_{\mathrm{Mu}}=(\tfrac{1}{2}s^2)f_{\mathrm{Mu}}[1-\exp(-K_S\tau_c)] ,$$
$$P^2_{\mathrm{Mu}}=P^4_{\mathrm{Mu}}=(\tfrac{1}{2}c^2)f_{\mathrm{Mu}}[1-\exp(-K_S\tau_c)] , \tag{4.1}$$

$$P_\mu=f_\mu+f_{\mathrm{Mu}}\exp(-K_S\tau_c) . \tag{4.2}$$

The sum of the polarizations is unity. That is, there is no lost fraction. Thus no depolarization occurs at these high number densities and the amplitudes are equal to the fractions defined by Eq. (2.14). In contrast, f_{Mu} and f_μ are the fractions of muonium and muon, respectively, that emerge from the charge exchange region at high densities when $K_S\tau_c\gg1$. That is, they are the appropriate chemical kinetic fractions.

V. LARGE RATE-CONSTANT EXPRESSIONS

When the time duration of the charge exchange regime is such that $K_S\tau_c\gg1$ while (ω_0/R_S) is small but finite, then spin depolarization can occur. In particular, if $\omega_0^2/f_\mu R_S\ll1$, then only one root will contribute to the amplitudes as the second and third relaxation rates will lead to large exponential damping. Such situations require large rate constants if they are to be valid over the number-density region of experimental interest. Otherwise the exact expressions must be used. To second order in (ω_0/R_S) the relaxation rate and frequency, for the s root, are

$$\lambda_{S,1}=s^2\omega_0^2[1-s^2f_{\mathrm{Mu}}(1+f_\mu)]f_{\mathrm{Mu}}/f_\mu R_S$$
$$=s^2\omega_0^2[\lambda_1-s^2\lambda_2]/(nK_S)^2 \tag{5.1}$$

and

$$\nu_{S,1}=-s^2\omega_0^2f_{\mathrm{Mu}}/nK_S , \tag{5.2}$$

respectively. Similar expressions hold for the c roots. The amplitudes of the resolved paramagnetic signals, Eq. (3.7) and (3.10), are then dominated by the following expressions:

$$P^1_{\mathrm{Mu}}=P^3_{\mathrm{Mu}}=s^2f_{\mathrm{Mu}}\exp[-s^2(\lambda_1-s^2\lambda_2)\omega_0^2\tau_c/K_Sn^2]$$
$$P^2_{\mathrm{Mu}}=P^4_{\mathrm{Mu}}=c^2f_{\mathrm{Mu}}\exp[-c^2(\lambda_1-c^2\lambda_2)\omega_0^2\tau_c/K_Sn^2] . \tag{5.3}$$

Associated with the first signals is the phase $\varphi_\mu-s^2f_{\mathrm{Mu}}\omega_0\tau_c/n$, while the second signals involve the phase $\varphi_\mu+c^2f_{\mathrm{Mu}}\omega_0\tau_c/n$. Thus the resolved signals exhibit simple exponential damping along with strongly time-dependent phases. On the other hand, for low fields where $c=s$, $\lambda=\lambda_1-\frac{1}{2}\lambda_2$ and where Ω is not resolvable, the phases of the triplet and singlet signals are constant, while the amplitudes

$$P_{\mathrm{Mu}}=P^0_{\mathrm{Mu}}=\tfrac{1}{2}f_{\mathrm{Mu}}\exp(-\tfrac{1}{2}\lambda\omega_0^2\tau_c/K_Sn^2)\times|\cos(\tfrac{1}{2}f_{\mathrm{Mu}}\omega_0\tau_c/n)| \tag{5.4}$$

exhibit resonances. The periods of these resonances, $t_0=\frac{1}{2}f_{\mathrm{Mu}}t_c=\pi(2m+1)/\omega_0=0.055\times(2m+1)$ nsec (m is an integer), occur at $\frac{1}{2}f_{\mathrm{Mu}}$ times the periods of the hyperfine interaction. That is, the periods are determined by the "fraction" of time, $\frac{1}{2}f_{\mathrm{Mu}}t_c$, that the muon spends in the singlet muonium state. The resonances are a quantal interference effect for the large rate-constant limit. Finally the diamagnetic amplitude, Eq. (3.18), becomes

$$P_\mu=f_\mu\exp\{-\tfrac{1}{2}\omega_0^2\tau_c[\lambda_1-(s^2+c^2)\lambda_2]/K_Sn^2\}(\cos^2(\tfrac{1}{2}f_{\mathrm{Mu}}\omega_0\tau_c/n)+\sinh^2\{\tfrac{1}{2}\omega_0\tau_c[\lambda_1(c^2-s^2)-(c^4-s^4)\lambda_2]/K_Sn^2\})^{1/2} . \tag{5.5}$$

The exponential decay of both the paramagnetic and diamagnetic signals involves the inverse of the product of the total rate constant and the square of the number density. This is the only place that the total rate enters these large rate expressions. Thus exponential damping will only occur for small number densities.

VI. FITS TO NOBLE-GAS EXPERIMENTS

Fits of the above expressions, Eqs. (3.18) and (3.19), for the diamagnetic muon and triplet muonium amplitudes are now made to the available experimental data for the noble gases. The theoretical line shapes describe the normalized amplitudes of the μSR signals, Eq. (2.5), as a function of the time duration of the charge exchange regime and are to be compared to the experimental amplitudes or asymmetries divided by the absolute aluminum asymmetry. Since the time duration t_c of the charge exchange regime is inversely proportional to the number density of the moderating gas, the line shapes are depicted here as a function of the number density. Indeed, as the experiments have all been run at room temperature, then the number density is simply proportional to the pressure which represents the experimental variable. Both the diamagnetic muon and triplet muonium amplitudes must be fit with consistent sets of parameters. The parameters to fit are the total rate constant, $K_S = K_L + \frac{1}{2}K_C$, the muon fraction $f_\mu (= 1 - f_{\mathrm{Mu}})$, and the time duration τ_c.

A. Argon

Muon and muonium amplitudes in pure argon have been observed at TRIUMF[2,4] and at SIN (Schweizerisches Institut für Nuklearforschung)[5]. For pressures greater than 1 atm the diamagnetic muon amplitude has a constant value of 0.24, whereas the muonium amplitude is gradually increasing up to 3 atm. Various fits can be made to both the muon and muonium amplitudes which represent the data equally well. For the diamagnetic signal, these fits all have the same fraction of muon, namely, $f_\mu = 0.24$ and the same duration of the charge exchange regime $\tau_c = 1.3/\omega_0 = 0.046$ nsec atm. However, there is only a lower limit on the total rate constant K_S, namely, $15.0\omega_0 = 4.2 \times 10^{11}$/sec. Two illustrative fits are shown. In the first, see Fig. 1 the lower limit on K_S has been assumed. The squares represent the TRIUMF data, with the remainder being the SIN data. For this fit the resonances are not experimentally resolvable. In Fig. 2 the corresponding paramagnetic muonium amplitudes are plotted for the same set of parameters. Here the data

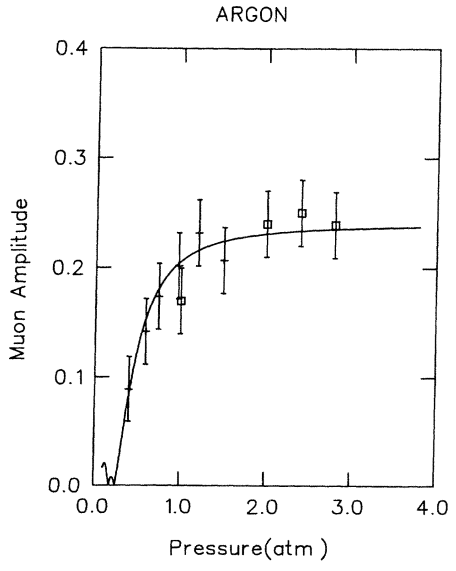

FIG. 1. Muon amplitude for argon. The points given with a box in this figure and in Figs. 2–12 are TRIUMF data, while the remainder are from SIN. The parameters for this line shape and those of Figs. 2 and 3 are $K_S = 15.0\omega_0$, $f_\mu = 0.24$, and $\tau_c = 1.3/\omega_0$.

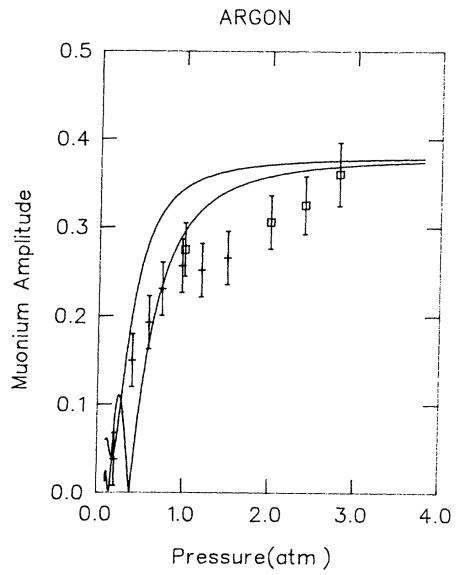

FIG. 2. Muonium triplet and singlet amplitudes for argon. The triplet line is the upper one at large pressures.

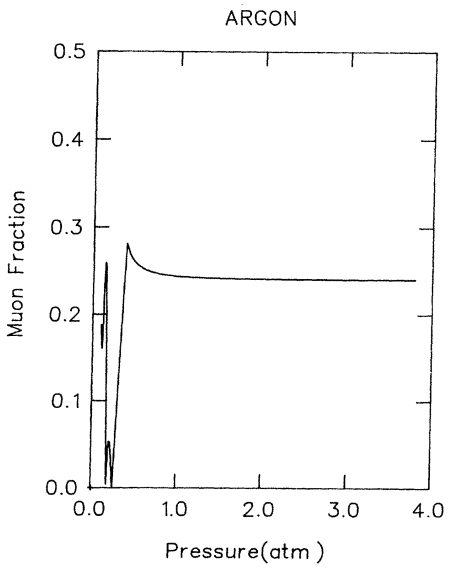

FIG. 3. Fraction of muon for argon.

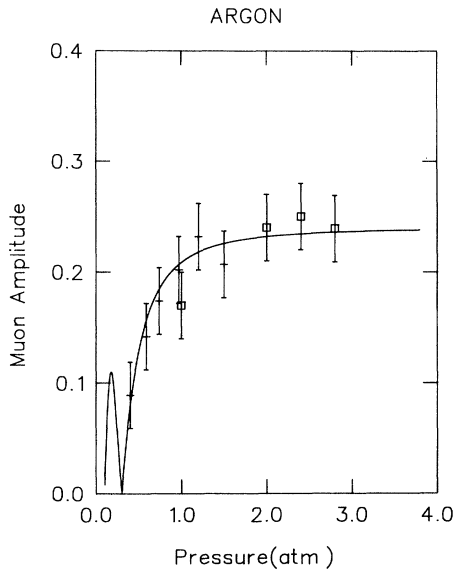

FIG. 4. Muon amplitude for argon. The parameters for this line shape and those of Figs. 5 and 6 are $K_S=50\omega_0$, $f_\mu=0.24$, and $\tau_c=1.3/\omega_0$.

points are the experimentally observed triplet amplitudes while the largest line shape at high pressures is the triplet signal obtained from theory. Clearly the predicted triplet and singlet amplitudes are not equal. Although this representation of the data is not very good it is not grossly in error. Finally, in Fig. 3 the fraction of muon, Eq. (2.14), is plotted for this fit. The other fit to the muon signal presented here has $K_S=50\omega_0=14\times10^{11}$/sec. This choice is somewhat arbitrary but does demonstrate the general features of the predicted line shapes for large rate constants. In particular, the resonances predicted for both the diamagnetic signal, see Fig. 4 and the triplet signal, see Fig. 5, are experimentally resolvable. Also the singlet and

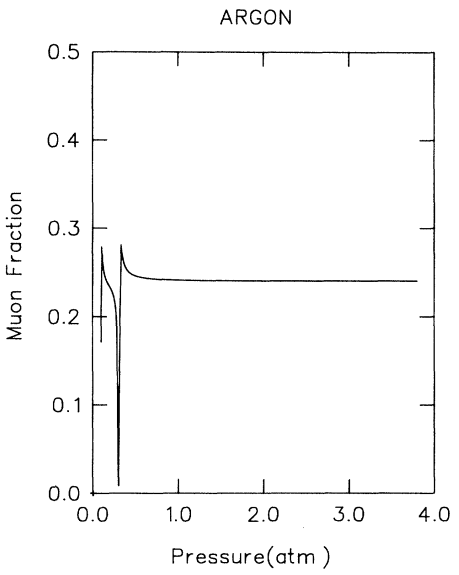

FIG. 6. Fraction of muon for argon.

triplet line shapes are essentially equal. The muon fraction is given in Fig. 6.

On the other hand, it is also possible to fit the triplet signal and then compare the results to the diamagnetic signal. Again, two types of fits are possible, that is, one with experimentally resolvable resonances and one without. These fits have essentially the same form as the muon fits. However, the predicted muon line shapes are worse than the predicted triplet line shapes from the muon fits. A triplet fit is presented in Fig. 7 whose associated parameters are $K_S=16\omega_0=4.5\times10^{11}$/sec, $f_\mu=0.39$, and $\tau_c=1.7/\omega_0=0.061$ nsec atm. The corresponding muon line shape is given in Fig. 8. A comparison of Figs. 2, 5, and 8 suggests that either the finite-width-step-function

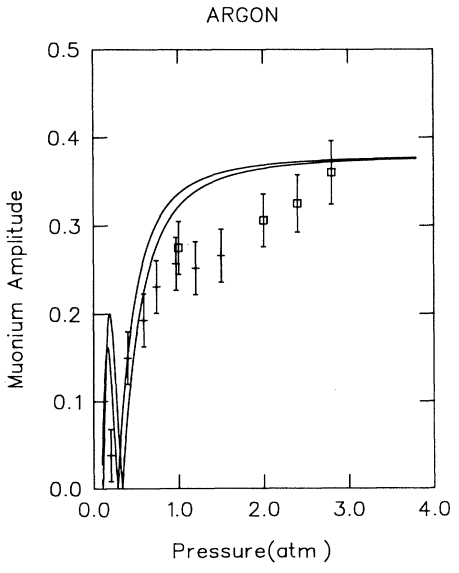

FIG. 5. Muonium triplet and singlet amplitudes for argon. The triplet line is the upper one at high pressures.

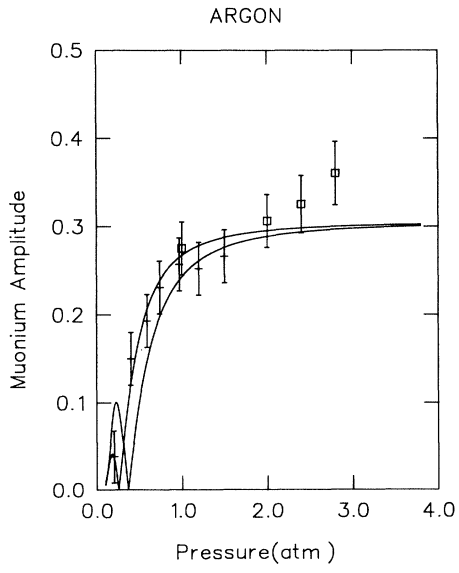

FIG. 7. Muonium triplet and singlet amplitudes for argon. The upper line at high pressures is again the triplet signal. The parameters for these lines and Fig. 8 are $K_S=16\omega_0$, $f_\mu=0.39$, and $\tau_c=1.7/\omega_0$.

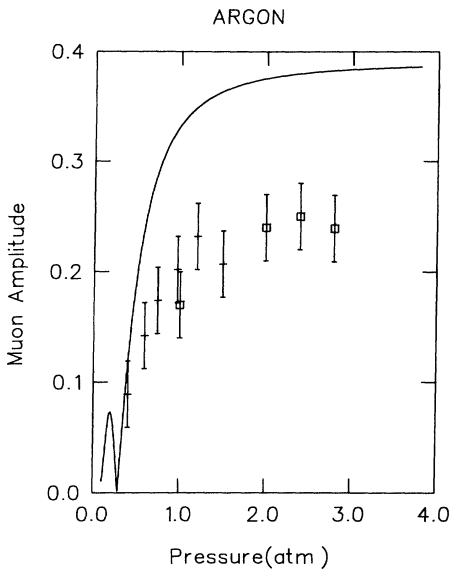

FIG. 8. Muon amplitude for argon.

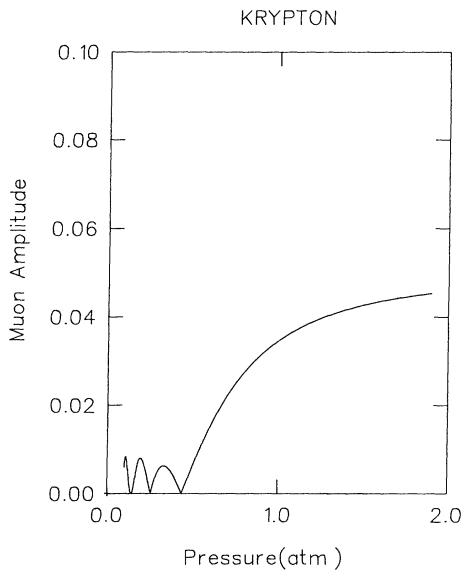

FIG. 10. Muon amplitude for krypton. This is the predicted muon line shape obtained from the parameters of the muonium fit.

approximation is inadequate or the experimental triplet amplitudes between 1 and 3 atm are too low.

B. Krypton and xenon

Muon and muonium amplitudes have also been measured in pure krypton and xenon at TRIUMF[2,4] and SIN.[5] The triplet muonium amplitudes are very similar for both gases, while the diamagnetic muon amplitudes are less than 0.05 for all pressures that have been measured. This latter result forces an upper limit on the muon fraction, namely, that f_μ be less than or equal to 0.05. Fits to the triplet krypton and xenon amplitudes with this constraint are not very good. The major problem in fitting the data is that the theoretical line shapes are too large at high pressures. However in light of the argon results where, again, there is a discrepancy at high pressures, the above results for krypton and xenon are not unreasonable. Representative fits for both krypton and xenon are presented in Figs. 9–12. The parameters for the krypton fit are $K_S=47.0\omega_0=13\times10^{11}$ sec, $f_\mu=0.05$, and $\tau_c=1.5/\omega_0=0.054$ nsec atm, while those for the xenon fit are $K_S=30.0\omega_0=8.4\times10^{11}$ sec, $f_\mu=0.05$, and $\tau_c=1.6/\omega_0=0.057$ nsec atm. There is very little difference between these two sets of parameters which, again, is indicative of the close resemblance of the experimental amplitudes.

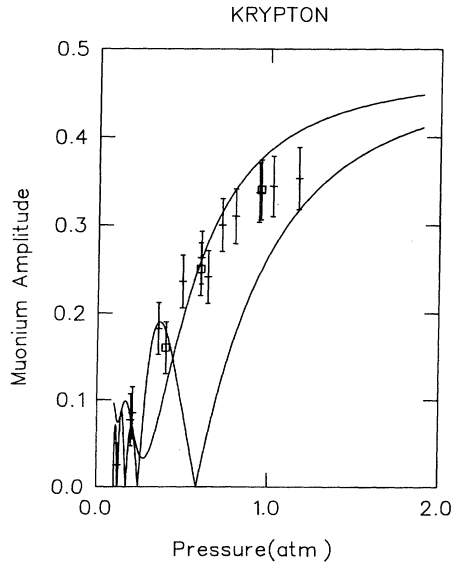

FIG. 9. Muonium amplitude for krypton. The parameters for these line shapes are $K_S=47.0\omega_0$, $f_\mu=0.05$, and $\tau_c=1.5/\omega_0$. The upper line at high pressures is the triplet signal.

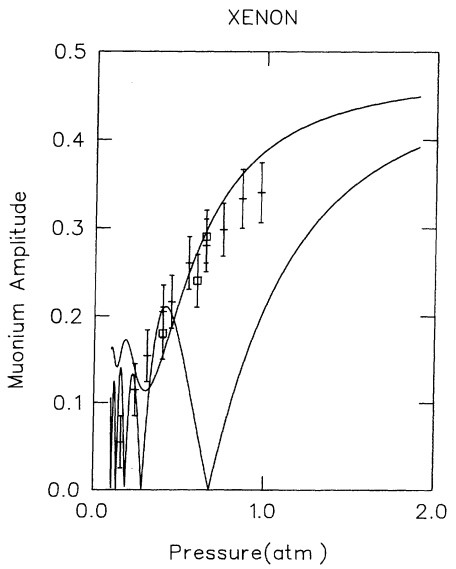

FIG. 11. Muonium amplitude for xenon. The parameters for these line shapes are $K_S=30.0\omega_0$, $f_\mu=0.05$, and $\tau_c=1.6/\omega_0$. The upper line at high pressures is the triplet signal.

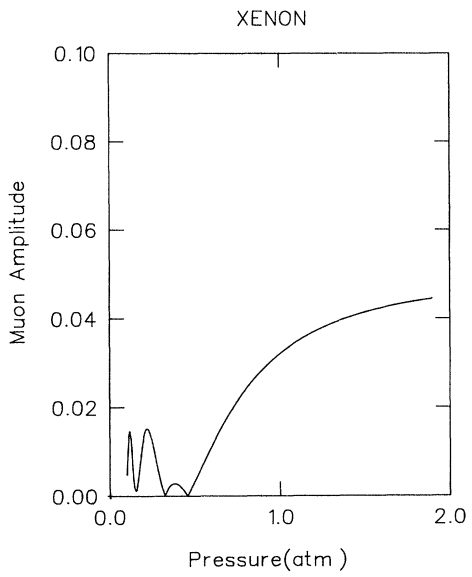

FIG. 12. Muon amplitude for xenon. This is the predicted muon line shape obtained from the parameters of the muonium fit.

VII. DISCUSSION

An approximation to the spin dynamics associated with the stopping process of highly energetic muons in single-component gases has been presented in which the time-dependent rates for electron capture and loss have been replaced by finite-width step functions of different heights but equal widths, namely, the duration of the charge exchange regime t_c. Expressions for the diamagnetic muon and paramagnetic muonium amplitudes have been obtained as a function of t_c. The resulting line shapes have two general features, namely, they are constant at short times and exhibit resonances at long times. Also in general, the triplet and singlet muonium amplitudes are not equal. Neither the possible resonances nor the difference between the triplet and singlet amplitudes have been observed experimentally. However, the theoretical line shapes obtained for argon, krypton, and xenon are in reasonable agreement with the experimental data. This suggests that the finite-width-step-function approximation is not unreasonable, at least, as a first approximation. Finally, the discrepancies at high pressures and the possibilities of observable resonances at low pressures suggest that further experiments be carried out as a test of the theory.

[1]D. G. Fleming, D. M. Garner, L. C. Vaz, D. C. Walker, J. H. Brewer, and K. M. Crowe, Adv. Chem. Phys. 175, 279 (1979).
[2]D. G. Fleming, R. J. Mikula, and D. M. Garner, Phys. Rev. A 26, 2527 (1982).
[3]R. E. Turner, Phys. Rev. A 28, 3300 (1983).
[4]R. J. Mikula, Ph.D. thesis, University of British Columbia, 1981 (unpublished).
[5]K. P. Arnold, Diplomarbeit, Universität Heidelberg, 1980 (unpublished).
[6]P. W. Percival, E. Roduner, and H. Fischer, Chemical Physics 32, 353 (1978).
[7]P. W. Percival, Hyperfine Interact. 6, 373 (1979); Radiochim. Acta. 26, 1 (1979); J. Chem. Phys. 72, 2091 (1980).
[8]D. C. Walker, Y. C. Jean, and D. G. Fleming, J. Chem. Phys. 70, 4534 (1979); 72, 2902 (1980).
[9]B. C. Sanctuary and R. F. Snider, J. Chem. Phys. 55, 1555 (1971).
[10]K. Huang, *Statistical Mechanics* (Wiley, New York, 1963).
[11]R. G. Newton, *Scattering Theory of Waves and Particles* (McGraw-Hill, New York, 1966).
[12]M. Baranger, Phys. Rev. 111, 495 (1958).
[13]F. Reif, *Fundamentals of Statistical and Thermal Physics* (McGraw-Hill, New York, 1965).